NASA-CR-196023

p 24

INTERIM REPORT

NASA CONTRACT NAG5-1049
June 14, 1994

Submitted by
Raj C. Yalamanchili

DEPARTMENT OF ELECTRICAL ENGINEERING
SCHOOL OF ENGINEERING
HOWARD UNIVERSITY
WASHINGTON, D.C.

(NASA-CR-196023) INTERIM REPORT (Howard Univ.) 24 p

N94-72098

Unclas

Z9/32 0012574

This INTERIM REPORT deals with only one of the three aspects of research at Howard University: Microstrip Antenna. The other two aspects are: Superconducting Waveguides and Fiber Optics. These will be included in the Final Report.

We have published one paper entitled "Review of Microwave Distributed Superconducting Vortex-Flow Transistor Amplifier". in the International Journal of Electronics, vol.73, no.3, pp 585-604,1992.

Two other papers are accepted for publication in June 1994 in the same Journal. The titles of these papers are:

1." Scattering by the Transition Junction between a Conventional and a High Temperature Superconducting Waveguides". Acceptance Ref. no. 84812

2."Meissner Model of Superconducting Rectangular Waveguides". Acceptance Ref. no. 84813.

The following paper was sent recently for publication in the Journal of Applied Physics:

"Rectangular Waveguides with two Conventional and two Superconducting Walls"

One of the students supported by this project received her M.S.E.E. degree in December 1993. Two more students will be graduating with M.S.E.E. degrees by the end of July 1994.

CONTENTS

Introduction

i. Purpose of Study . . . . . (3)
ii. Statement of the Problem . . . . . (3)

I. General Theory - The Cavity Model . . . . . (4)

i. Rectangular Patch Antennas . . . . . (9)
ii. Circular Patch Antennas . . . . . (11)

II. Software Interfaces . . . . . (12)

i. Conventional Programming . . . . . (12)
ii. User - friendly Packages . . . . . (12)

III. Proposed Experimental Testing . . . . . (13)

i. Network Analyzer Testing . . . . . (13)
ii. Anechoic Chamber Testing . . . . . (14)

IV. Conclusions . . . . . (14)

References . . . . . (15)

INTRODUCTION

The small physical sizes of microstrip antennas allow them to be conformally fit into certain physical areas in missile cones, air - craft, spacecraft, etc.

Microstrip patch antennas may be shaped in the form of rec - tangular, circular , annular ring , triangular , elliptical , or spherically-cut geometrical sections.

Most of the studies were done on the rectangular and circular patch antennas. The rigorous mathematical equations associated with rectangular and circular patch antennas have been most useful , since these shapes are not irregular; besides, applications for these antennas extend well beyond those of antennas possessing irregular shapes.

Input impedance characteristics (analysis by Smith Chart) are also easily verified by use of the Network Analyzer. Anechoic Chamber testing of actual microstrip antennas can provide verification of the derived radiated field quantities.

i. Purpose of Study

The overall purpose is to gain knowledge of the microstrip patch antenna in the form of rectangular and circular contours for thin substrate antennas. Since the applications include aircraft and aerospace uses (at microwave frequencies) , electromagnetic field equations which are easily programmable are contained herein. Another purpose involves showing that the analyses of these configurations are achievable and practical.

Applicability of the study is to be determined by NASA and the author's advisor, Dr. Raj C. Yalamanchili, Chairman of Electrical Engineering Graduate Studies, Howard University.

ii. Statement of the Problem

An illustration of various microstrip antenna configurations is shown in figure 1. The rectangular patch configuration will be emphasized in this paper; however, the circular patch antenna also will be discussed.

A general discussion of the Cavity Model begins, with some model parameter restrictions given. Then, field quantities in between the conducting plates ("under the patch") are shown such that free-space radiated fields and patch impedances are obtained.

Even though similar, both rectangular and circular patch configuration details are provided such that differentiation between both of these configurations is possible.

Computer calculations of mathematical results and proposed microstrip antenna testing are included in this report.

Figure 1

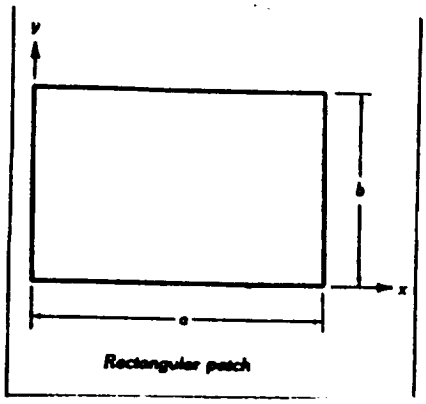

Rectangular patch

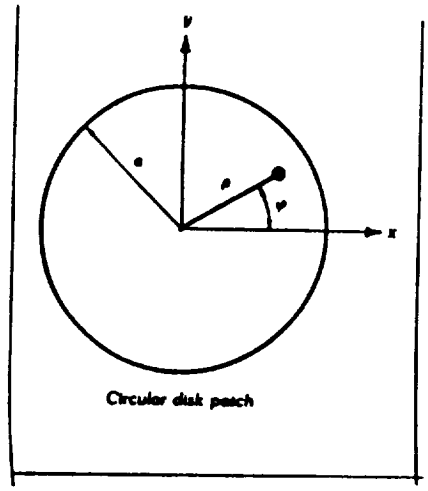

Circular disk patch

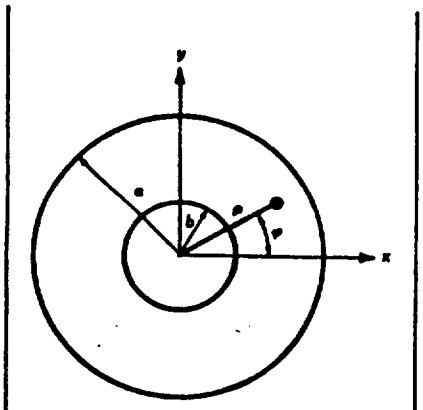

Annular patch

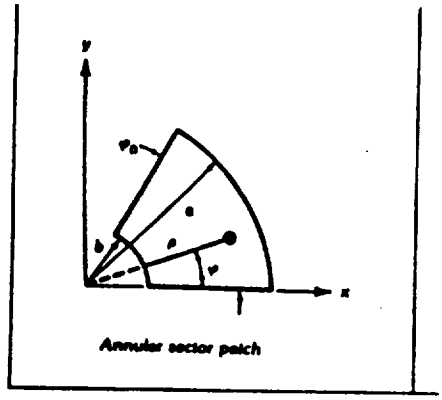

Annular sector patch

I. GENERAL THEORY - THE CAVITY MODEL

The basic configurations for rectangular and circular patch antennas is shown in figure 2. The Cavity Model is used for thin substrates , such that : $d \leq 0.01\ \lambda_o$, where

d = substrate thickness ; λ_o = free-space wavelength

The main principle of understanding the Cavity Model is that the upper and lower conductors (patch and ground plane, respectively) serve as electric walls, whereas the side walls behave as theoretical magnetic, or " H-walls ". Therefore, the configuration is seen as a cavity enclosure - hence, the name " Cavity Model ".

Certain assumptions must exist in order for the Cavity Model to be used:

(1) The E-field under the patch has a z-component only , due to close proximity of the upper conductor to the ground plane ,

(2) The H-field has only transverse components in the region betweeen the conductor plates (for $0 < z < d$) ,

(3) The partial derivative of E_z or H_z with respect to the outer H-wall normal vector is zero, for all frequencies of interest for $0 < z < d$ (these are the boundary conditions) ,

(4) The H-field tangential component along the patch edge is negligible, meaning that the electric current in the microstrip has no component normal to the edge at any point on the edge, and

(5) The region $0 < z < d$ can be seen as a cavity bounded by magnetic walls on the outer edges, and by electric walls from above and below (top and bottom conductor plates).

In general, the electric-field and magnetic field components are of the following form (see page 5) :

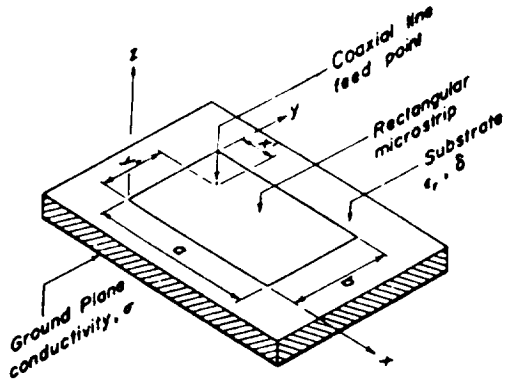

Rectangular microstrip antenna.

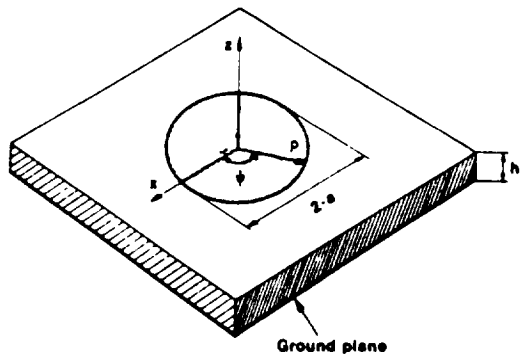

Circular microstrip disk antenna element.

Figure 2

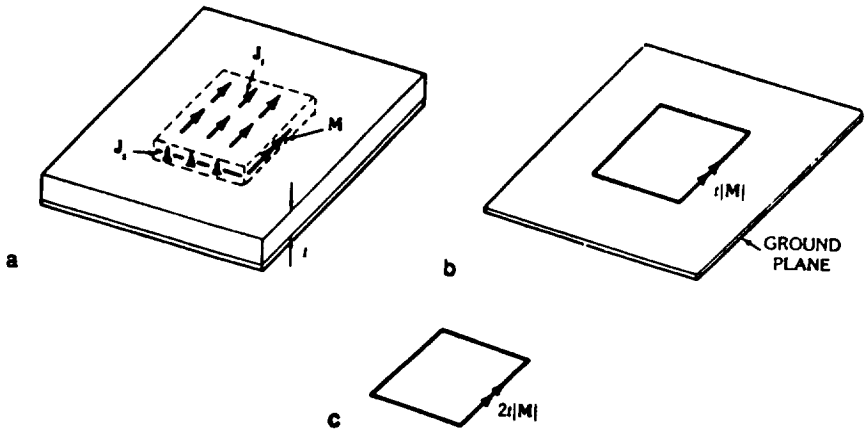

Source modeling for pattern computations. (*a*) Exact model for the exterior field of a microstrip antenna in terms of equivalent electric and magnetic current. (*b*) Approximate model with the dielectric removed, the electric currents ignored, and the magnetic current condensed to a filamentary magnetic current of strength equal to $t|\mathbf{M}|$. (*c*) Equivalent approximate model with the ground plane removed.

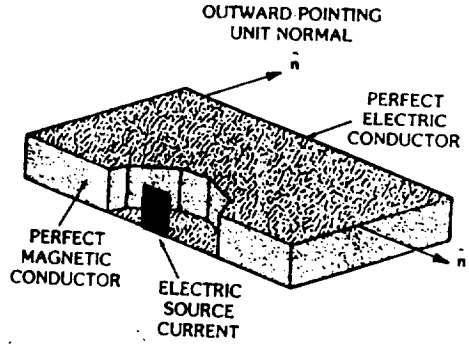

Figure 4

Figure 3

4-1

$$\vec{E}_z = \psi_m \vec{z} \tag{1}$$

$$\vec{H} = \frac{\vec{z} \times \nabla_t \psi_m}{j\omega\mu} \tag{2}$$

where ω = angular frequency, in radians

$\mu = \mu_o$ = free-space permeability ($4\pi \times 10^{-7}$, Henries/meter)

ψ_m = modal solutions meeting the boundary conditions

∇_t = transverse del operator, transverse to the z-direction

The Helmholtz Equation and boundary conditions to be satisfied are:

$$(\nabla_t^2 + k_m^2) \psi_m = 0 \tag{3}$$

$$\frac{\partial \psi_m}{\partial n} = 0 \tag{4}$$

(on the magnetic walls)

As will be seen later, the modal solutions for the field quantities change with respect to the patch shape chosen.

Referring to figure 3 , the equivalent magnetic circuit is taken to be a magnetic ring for which the Huygen's magnetic source vector can be obtained :

$$\vec{K}_p = 2\vec{n} \times \vec{z}E_z \tag{5}$$

where p = 1, 2, 3, or 4 for a rectangular patch , and p = r (radial) for a circular patch. The outward normal vector to the H-wall is the " n" vector. The factor of two accounts for the ground plane existence.

Referring to figure 4, these quantities were obtained with respect to the four individual sidewall outer normal vectors, for the

rectangular case and with respect to the outer radial vector for the circular case.

After the K_p's are obtained, vector potential quantities can be obtained according to the following formula :

$$F(r) = \frac{\epsilon_0 e^{-jk_0 r}}{4\pi r} \int_{v'} e^{jk_0 [x' Sin\theta Cos\phi + y' Sin\theta Sin\phi + z' Cos\theta]} \, dV' \qquad (6)$$

After these vector potential quantities are known, the spherical-coordinate radiated field quantities can be derived, since :

$$E_\theta = \frac{jk_0 F_\phi}{\epsilon_0} \qquad (7)$$

$$E_\phi = \frac{-jk_0 F_\theta}{\epsilon_0} \qquad (8)$$

From these components the power radiated due to the electric field components under the patch is :

$$P_r = \frac{1}{\eta_0} \int_0^{\pi/2} \int_0^{2\pi} [\, |E_\theta|^2 + |E_\phi|^2 \,]^2 r^2 Sin\theta \, d\phi \, d\theta \qquad (9)$$

The power values due to the surface conductors and the dielectric are to be calculated next. In the Cavity Model, surface waves are negligible; therefore, surface wave power is taken to be zero due to the thin substrate.

Also, the electric energy stored under the patch must be calculated. The power due to the dielectric, and that of the conductors , are :

$$P_d = \frac{1}{2}\int_V [\ \sigma_d |E_z|^2\ ]\ dV$$
$$= \frac{\sigma_d W_E}{\epsilon_r \epsilon_0} \qquad (10)$$

$$P_c = \sqrt{\frac{\pi f_r \mu_0}{\sigma_c}} \int_S |H|^2\ dS$$
$$= 2\sqrt{\frac{\pi f_r \mu_0}{\sigma_c}}\ \frac{W_E}{d} \qquad (11)$$

, where the electric energy stored under the patch is :

$$W_E = \frac{1}{2}\epsilon_r \epsilon_0 \int_V |E_z|^2\ dV \qquad (12)$$

The conductor surface resistance is:

$$R_S = \sqrt{\frac{\omega \mu_0}{2\sigma_c}} \qquad (13)$$

where d = substrate thickness, σ_d = dielectric conductivity $(2\pi f_r \epsilon_r \epsilon_o)$, σ_c = conductor surface conductivity , and f_r = the patch resonant frequency.

These values are needed to obtain a quality factor , Q , for each power relation above. In general , $Q = (2\pi W_E f_r / P)$ **(13a)** where P is the type of power to be calculated (surface, radiated, dielectric or conductor power). The separate types of quality factors needed (neglecting surface wave contributions) are as follows :

$$Q_d = (\ 2\pi f_r \epsilon_r \epsilon_o / \sigma_d\ ) = (2\pi f_r\ W_E / P_d) \approx (\ 1 / \tan\delta\ ) \qquad (13b)$$

where $\tan\delta$ is the loss tangent of the dielectric substrate.

$$Q_c = d(\mu_o \pi f_r \sigma_c)^{1/2} \qquad (13c)$$

$$Q_{rad} = (\ 2\pi f_r W_E / P_r\ ) \qquad (13d)$$

and : $1/Q_{TOT} = [\ 1/Q_{rad} + 1/Q_c + 1/Q_d\ ]$ **(13e)**

If the source used is a probe (coax) feed line , then the patch fields are modified , and equation **(3)** becomes inhomogeneous (the right side is no longer = 0) . Therefore, the new electric field quantity under the patch is augmented , such that :

$$E_z = jk_0\eta_0 \sum_{m=0}^{\infty}\sum_{n=0}^{\infty} \frac{\Phi^2_{mn}\ j_0^2(m\pi d/2a)}{k^2 - k_{mn}^2} \qquad \textbf{(14)}$$

where ,

$k^2 = \epsilon_r\ (1-j\delta)\ (k_0)^2$ = square of the complex dielectric wave number

$k_o = \omega\ /\ v$ = free-space wave number (v = wave velocity)

k_{mn} = patch modal wave number
$= [(m\pi/a)^2 + (n\pi/b)^2]^{1/2}$ - for a rectangular patch
$= (\alpha_{mn}\ c\ /\ 2\pi a(\ \epsilon_r\ )^{1/2}$ - for a circular patch

$j_0(x) = \sin(x)\ /\ x$

c = speed of light

α_{mn} = mth zero of $J'_N(z)$ Bessel Function of the First Kind , of order N (for the circular patch)

The Cavity Model requires that the loss tangent parameter δ be set equal to an effective loss tangent value, δ_{eff} . In turn , $\delta_{eff} = (1\ /\ Q_{TOT})$. After several manipulations, the value of the patch impedance is :

$$Z = \frac{j\omega\mu_0 dv^2}{e_r} \sum_{m=0}^{\infty}\sum_{n=0}^{\infty} \frac{\Phi_{mn}^2\ j_0^2(m\pi d/2a)}{\omega_{mn}^2 - (1-j\delta_{eff})\,\omega^2} \qquad \textbf{(15)}$$

where $\omega_{mn} = (\ v\ k_{mn}\ )\ /\ (\epsilon_r)^{1/2}$, and $\omega = 2\pi f$ and ϵ_r is the relative dielectric constant of the substrate. The impedance locus of the microwave S-parameter S_{11} can be obtained (w/ Z_o , the characteristic -

impedance of the matching transmission line, 50 ohms) by the relation :

$$S_{11} = (Z - Z_o) / (Z + Z_o)$$

Examples of typical impedance loci can be found in figure 5 for the rectangular patch configuration.

i. **Rectangular Patch Antennas**

For a rectangular patch antenna, the modal fields under the patch which meet the boundary conditions are :

$$E_z = V_o \, Cos(m\pi x/a) \, Cos(n\pi y/b)$$

$$H_x = -(j\omega\epsilon_o / (k_o)^2)(n\pi/b)(V_o/d) \, Cos(m\pi x/a) \, Sin(n\pi y/b)$$

$$H_y = (j\omega\epsilon_o \, m\pi \, V_o / (k_o)^2 \, a \, d) \, Sin(m\pi x/a) \, Cos(n\pi y/b)$$

and, $f_r = (c/2 \, (\epsilon_r)^{1/2}) \, [(m/a)^2 + (n/b)^2]^{1/2}$, where V_o is the peak voltage at the corner of the patch. Letting $(V_o / d) = E_o$ = constant , and also referring to equation **(5)** and figure 3 , the magnetic vector quantities become :

$$\vec{K}_1 = \vec{y} \, 2E_o Cos(n\pi y/b) \, \delta(x) \, \delta(z) \qquad \textbf{(16)}$$

$$\vec{K}_2 = \vec{x} \, 2E_o Cos(m\pi x/a) \, Cos(n\pi) \, \delta(y-b) \, \delta(z) \qquad \textbf{(17)}$$

$$\vec{K}_3 = -2\vec{y} \, E_o Cos(m\pi) \, Cos(n\pi y/b) \, \delta(x-a) \, \delta(z) \qquad \textbf{(18)}$$

$$\vec{K}_4 = -2\vec{x} E_o Cos(m\pi x/a) \, \delta(y) \, \delta(z) \qquad \textbf{(19)}$$

and $\delta(z)$ is a Dirac function used to account for the very thin substrate. Using equation **(6)** and equations **(7)** and **(8)** and ,

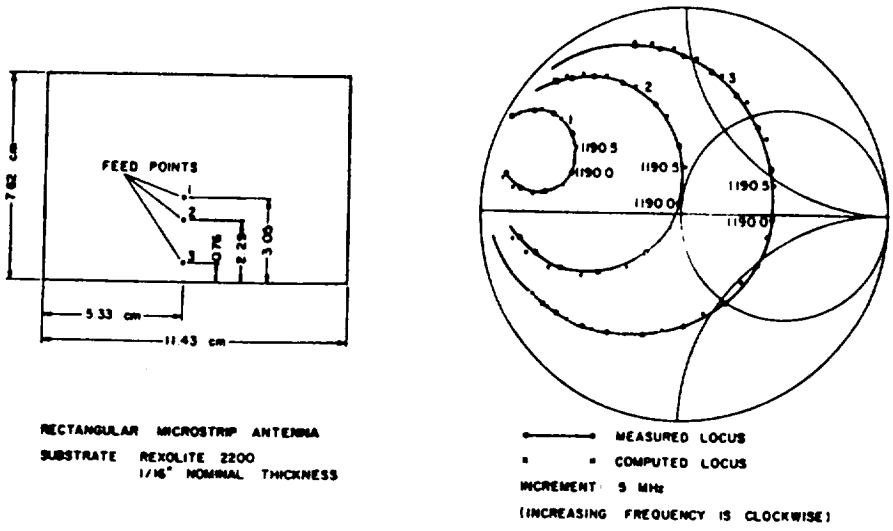
FEED POINTS
1
2
3
0.76 cm
2.29 cm
3.81 cm
7.62 cm
5.33 cm
11.43 cm
RECTANGULAR MICROSTRIP ANTENNA
SUBSTRATE REXOLITE 2200
1/16" NOMINAL THICKNESS
1190.5
1190.0
MEASURED LOCUS
COMPUTED LOCUS
INCREMENT 5 MHz
(INCREASING FREQUENCY IS CLOCKWISE)

Figure 5

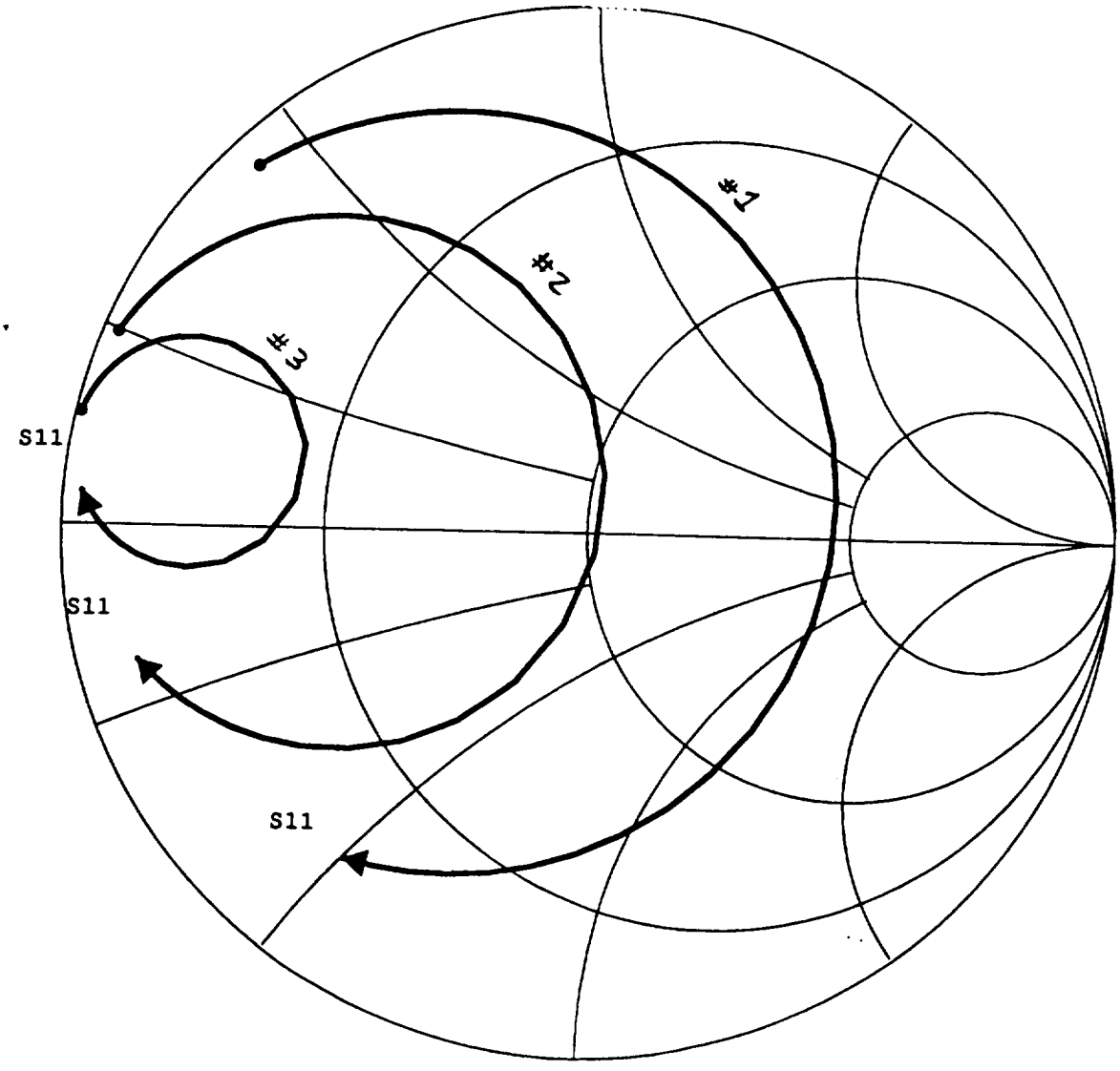
#1
#2
#3
S11
S11
S11

9A.

$$F_\phi = -F_x Sin\phi + F_y Cos\phi$$

$$F_\theta = F_x Cos\theta Cos\phi + F_y Cos\theta Sin\phi$$

and the radiated fields become :

$$E_\theta = -\frac{e^{(-jk_0 r)} 2V_0}{(2\lambda_0 r)} [1-Cos(m\pi)\, e^{(jk_0 a Cos\phi Sin\theta)}]\, [1-Cos(n\pi)\, e^{(jk_0 b Sin\phi Sin\theta)}]$$

$$x\ [k_0 Sin\theta Cos\phi Sin\phi]\ [[\frac{1}{(k_0 Cos\phi Sin\theta)^2 - (m\pi/a)^2} + \frac{(Cos\phi)^2}{(k_0 Sin\phi Sin\theta)^2 - (n\pi/b)^2}] \quad \textbf{(22)}$$

and,

$$E_\phi = \frac{e^{(-jk_0 r)} 2V_0}{(2\lambda_0 r)} [2V_0 k_0 Sin\theta Cos\theta]\, [1-Cos(m\pi)\, e^{jk_0 a Cos\phi Sin\theta}]\, [1-Cos(n\pi)\, e^{jk_0 b Sin\phi Sin\theta}]$$

$$x\ [\frac{(Sin\phi)^2}{(k_0 Sin\phi Sin\theta)^2 - (n\pi/b)^2} - \frac{(Cos\phi)^2}{(k_0 Cos\phi Sin\theta)^2 - (m\pi/a)^2}]$$

(23)

Using equation **(12)** for W_E, the energy stored under the rectangular patch becomes:

$$W_E = \frac{\epsilon_r \epsilon_0 V_0}{2d} \int_0^a \int_0^b (Cos(m\pi x/a))^2 (Cos(n\pi y/b))^2\, dx\, dy \quad \textbf{(24)}$$

$$= \frac{\epsilon_r \epsilon_0 (V_0)^2 ab}{2h} \delta_m \delta_n$$

where: $\delta_l = 1$, for $l = 0$
$= 1/2$, for $l = 1, 2, 3, \ldots$

From there, Z from equation **(15)** can be calculated.

An example of a Mathmatica 2.0 software package program which

calculates the various microstrip quantities discussed above appears in Section II, Part ii.

ii. **Circular Patch Antennas**

Using the modal patch equation (also see figure 6):

$E_Z(\rho=a) = E_0 \cos[N(\phi - \phi')] = (V_0/d) \cos[N(\phi - \phi')]$,

where the cylindrical coordinates used are r′, ϕ', and z′. The spherical coordinates used are r, ϕ, and θ. The vector potential integral for the circular patch becomes:

$$F(r) = \frac{\epsilon_0 e^{-jk_0 r} V_0 a}{2\pi r} \int_0^{2\pi} Cos(N(\phi'-\phi)) e^{jz Cos(\phi-\phi')} \vec{\phi} \; d\phi \qquad (25)$$

where $z = k_0 a \, Sin\theta$. Using the following relation to transform the cylindrical unit vector of equation **(25)** into spherical coordinates (such that the equation can be integrated properly):

$$\vec{\phi} = -Sin\theta Sin(\phi-\phi')\vec{r} + Cos\theta Sin(\phi-\phi')\vec{\theta} + Cos(\phi-\phi')\vec{\phi}$$

, for $\phi > \phi'$. After several manipulations, it is found that the radiated field components, in spherical coordinates are :

$$E_\theta = \frac{V_0 a \pi e^{-jk_0 r}}{\lambda_0 r} Cos(N(\phi-\phi') [J_{N+1}(z) - J_{N-1}(z)] e^{jN\pi/2}$$

$$E_\phi = -V_0 a \pi \frac{e^{-jk_0 r}}{\lambda_0 r} Sin(N(\phi-\phi')) [J_{N+1}(z) + J_{N-1}(z)] e^{jN\pi/2}$$

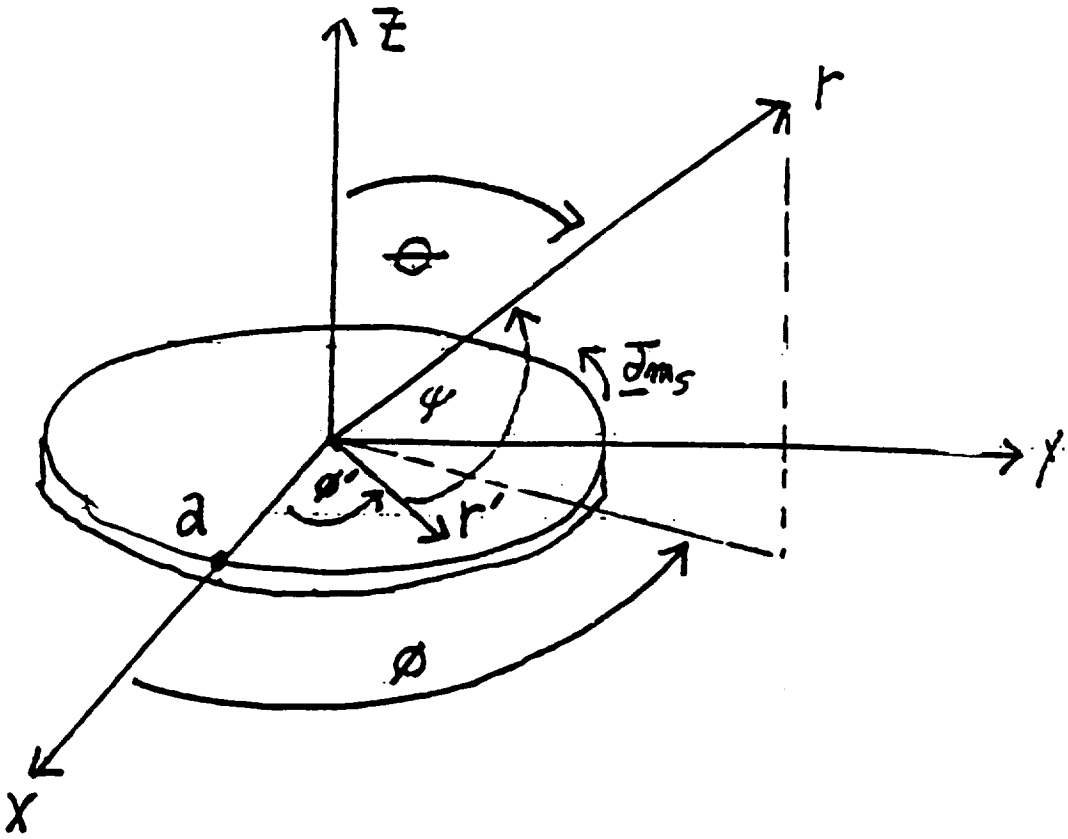

Figure 6. Circular patch configuration

Where $J_N(z)$ = Bessel function of the First Kind, of order N. The electric energy stored under the patch is (using equation **(12)**):

$$W_E = \pi (V_0)^2 \delta_N \frac{\epsilon_r (k_0)^2 a^2 - N^2}{2 d \omega^2 \mu_0}$$

The impedance can be found by the use of equation **(15)**, where

$$\Phi_{mn} = [(V_0/d) Cos(N(\phi - \phi'))]^2$$

II. SOFTWARE INTERFACES

i. Conventional Programming

Conventional programming would involve the use of computer languages such as Fortran, Basic, C, and Pascal. The use of the above languages is not advised, due to:

(1) Slow execution time (especially due to radiated power calculations)

(2) Requirement of long programming lines

ii. User - friendly Packages

User - friendly packages allow simpler use to perform complicated calculations. Since often the radiated power calculations slow down the execution time , the following software packages are recommended to rectify this:

(1) Matlab (2) Mathcad (3) Mathmatica

Mathmatica was used for the analysis of a rectangular patch sample. The run time for this type of programming is well under a minute.

Matlab Program
(Rectangular Patch Antenna)

```
<<Nodal2.m
```

(lamp0-jwhall) In[33]:=

```
a = 0.1143;
b = 0.0762;
x = 0.0533;
y = 0.0229;
Zo = 377;
cc = 3. 10^8;
uoo = 4 N[Pi] / 10^7;
eo = 8.854 / 10^12;
sigmaCu = 5.813 10^7;
deltaD = 0.001;
t = 0.1588 / 10^2;
er = 2.62;
m = 0;
n = 1;
f = 1.19 10^9;
```

(lamp0-jwhall) In[48]:=

```
ClearAll[fmn,kmn,wmn,  Koo,e,Emodal,SinC,alphamn,Etheta,Ephi]

fmn[m_,n_] = cc /2 / er^(1/2) ((m/a)^2+(n/b)^2)^(1/2);
kmn[m_,n_] = 2 Pi fmn[m,n] / cc;
wmn[m_,n_] = cc kmn[m,n] / er^(1/2);
Koo[f_] = 2 Pi f / cc //N ;
e[n_] :=1       /;    n==0
e[n_] :=2       /;    n!=0
Emodal[m_,n_] = Cos[m Pi x / a] Cos[n Pi y / b] *
(e[m] e[n] / (a b))^(1/2);

SinC[u_ /; u==0] := 1
SinC[u_ /; u!=0] := Sin[u]/u

alphamn[m_,n_] = t (Emodal[m,n])^2 / (er eo);


Etheta[theta_,phi_,m_,n_  /; (m == 0 && n == 1) ]  =
( SinC[  Koo[f] Sin[theta] Cos[phi] a/2] Sin[phi] a/2  +
Sin[  Koo[f] Sin[theta]Cos[phi] a/2]   Koo[f] Sin[theta]Sin[phi]Cos[p
(  Koo[f]^2 Sin[phi]^2 Sin[theta]^2 - (Pi/b)^2) )*
Cos[  Koo[f] Sin[theta] Sin[phi] b/2] //N;

Ephi[theta_,phi_,m_,n_ /; (m == 0 && n == 1) ]  =
( SinC[  Koo[f] Sin[theta] Cos[phi] a/2] Cos[phi] Cos[theta] a/2  -
(Sin[  Koo[f]Sin[theta]Cos[phi] a/2]  Koo[f]Sin[theta]Cos[theta] *
Sin[phi]^2) / (  Koo[f]^2 Sin[phi]^2 Sin[theta]^2 - (Pi/b)^2) )*
Cos[  Koo[f] Sin[theta] Sin[phi] b/2] //N        ;

Etheta[theta_,phi_,m_,n_ /; (m == 1 && n == 0) ]  =
Cos[  Koo[f] Cos[phi]Sin[theta] a/2] Sin[  Koo[f] Sin[phi]Sin[theta] ]
  Koo[f] Sin[theta] Cos[phi] Sin[theta] /
(  Koo[f]^2 Cos[phi]^2 Sin[theta]^2 - (Pi/a)^2 ) +
Cos[  Koo[f] Cos[phi]Sin[theta] a/2] SinC[  Koo[f] Sin[phi]Sin[theta]
Cos[phi] b/2  //N ;

Ephi[theta_,phi_,m_,n_ /; (m == 1 && n == 0) ]   =
Cos[  Koo[f]Cos[phi]Sin[theta] a/2]SinC[  Koo[f]Sin[phi]Cos[theta] b/
Cos[theta]Sin[phi] b/2 -  Cos[  Koo[f]Cos[phi]Sin[theta] a/2] *
Sin[  Koo[f]Sin[phi]Sin[theta] b/2]   Koo[f]Sin[theta]Cos[theta] *
Cos[phi]^2 /
(  Koo[f]^2 Cos[phi]^2 Sin[theta]^2 - (Pi/a)^2 ) //N;
```

(lamp0-jwhall) In[241]:=

```
ul = 5;
increment = 0.0025;
lower = 1.15;
upper = 1.25;

x = 0.0533;
y = 0.0305;
dataA = Table[ZZ[fff 10^9,ul,x,y], {fff,lower,upper,increment}] //N;
s11A = (dataA - 50)/ (dataA + 50);
plotA = SmithChart[s11A,DisplayFunction->Identity];

x = 0.0533;
y = 0.0229;
dataB= Table[ZZ[fff 10^9,ul,x,y], {fff,lower,upper,increment}] //N;
s11B = (dataB - 50)/ (dataB + 50);
plotB = SmithChart[s11B,DisplayFunction->Identity];

x = 0.0533;
y = 0.0076;
dataC = Table[ZZ[fff 10^9,ul,x,y], {fff,lower,upper,increment}] //N;
s11C = (dataC - 50)/ (dataC + 50);
plotC = SmithChart[s11C,DisplayFunction->Identity];


 Timing[integrand1 = NIntegrate[ (Ephi[theta,phi,m,n]^2 ) Sin[theta] ,
                          {theta,0, Pi/2}, {phi, 0, Pi/2}] ]

 Timing[integrand2 = NIntegrate[ (Etheta[theta,phi,m,n]^2 ) Sin[theta]
                          {theta,0, Pi/2}, {phi, 0, Pi/2}]  ]



 {18.7833 Second, 0.000684}

 {12.8 Second, 0.00122772}

 Pint = 4 ( integrand1 + integrand2 );
 Prad = N[8   Koo[f]^2 Pint / (Zo 4 Pi^2 )];
 Es = N[ er eo a b / (2 t e[m] e[n] ) ];


 Qd = 1/deltaD;
 Qcu = N[t ( uoo  Pi f sigmaCu )^(1/2)];
 Qr = N[2 Pi f Es / Prad ];
 Qtot = N[( Qd^-1 + Qcu^-1 + Qr^-1 )^-1];
```

(lamp0-jwhall) In[184]:=

```
a = 0.1143;
b = 0.0762;
x = 0.0533;
y = 0.0229;
t = 0.1588 / 10^2;
Qtot = 74.52913545364626;
pie = N[Pi];
```

(lamp0-jwhall) In[191]:=

```
ClearAll[ZZ,ffmn,kkmn,wwmn]

ffmn[m_,n_] := cc /2 / er^(1/2) ((m/a)^2+(n/b)^2)^(1/2);
kkmn[m_,n_] := 2 pie ffmn[m,n] / cc;
wwmn[m_,n_] := cc kkmn[m,n] ;


ZZ[f_,ul_,x_,y_]  := I 2 pie f  uoo  t cc^2 /er *
Sum[ Cos[mm pie x/ a]^2   Cos[nn pie y / b]^2  *
(e[mm] e[nn]/(a b)) /
( wwmn[mm,nn]^2 - (1 - I/Qtot) (2 pie f)^2 ),{mm,0,ul},{nn,0,ul}];
```

All sub - blocks of data individually were executed in a few seconds or less, with the exception of the radiated power calculations, which took closer to half of a minute to execute.

The parameters used as given input for the rectangular patch microstrip antenna were (for m=0 n=1 mode):

$a = 11.43$ cm.
$b = 7.62$ cm.
$\epsilon_r = 2.62$ cm.
$\tan\delta = 0.001$
$f_{01} = 1.19 \times 10^9$ Hz

these are the probe locations (source coordinates):

$x' = 5.33$ cm. ; $y' = 3.05, 2.29, 0.76$ cm.

The results are displayed in figure (5). The data shows that, for three different probe positions, impedance curve #2 is the best curve due to the fact that it intersects the $Z_0 = 50\Omega$ point in the middle of the Smith Chart. Therefore, the antenna impedance can be matched to a 50Ω transmission line source.

III. PROPOSED EXPERIMENTAL TESTING

i. Network Analyzer Testing

Once the computer verification of the antenna impedance locus data is known , the antenna can be coax-fitted below its ground plane surface such that it can be tested.

The Network Analyzer can be used to sweep frequencies near the resonant frequency of the antenna. It should be noted that no testing shall begin prior to calibration of the Network Analyzer.

ii. Anechoic Chamber Testing

The Anechoic Chamber provides a weatherproof means to test the antenna in its " quiet-zone ", which refers to the area of the test antenna isolated from extraneous reflected radiation. RF absorbers on the walls, ceiling, and floor help to attenuate any unwanted radiation that could reflect onto the test antenna.

The source antenna could be a standard horn antenna whose gain is known. Suggested tests include E-Plane , H-Plane , and the cross polarization tests. The data for these tests is recorded on machinery housed outside of the Anechoic Chamber (usually in a room adjacent to the chamber). The microstrip antenna can be rotated in various elevation and azimuthal angles (θ and ϕ) on its rotatable test stand inside of the chamber.

IV. CONCLUSIONS

Much can be gained from knowing how to design rectangular and circular patch microstrip antennas since they are the most commonly used configurations. Starting from theoretical design equations, one can obtain vital derivations that actually allow the prediction of radiated fields and impedance locus data. In this paper, the Cavity Model was the focus method since only thin-substrate microstrip antennas were discussed.

It was demonstrated that user-friendly software, such as the package " Mathmatica ", could be used in order to plot the impedance - locus data. Comparisons to figure (5) further illustrate this idea.

The proposed testing will simply serve as a means of verifying

additional data, including E and H - plane data, cross - polarization data, and Network Analyzer impedance locus verification.

REFERENCES

1.) Balanis, Constantine A., 'Antenna Theory', John Wiley and Sons, New York, 1982.

2.) Lo, Y.T., Solomon, D., and Richards, W.F., "Theory and Experiment on Microstrip Antennas", IEEE Transactions on Antennas and Propagation, AP-27, No. 2, March, 1979.

3.) Richards, William F., Lo, Yeun T., and Harrison, Daniel D., "An Improved Theory for Microstrip Antennas and Applications", IEEE Transactions on Antennas and Propagation, AP-29, No. 1, January, 1981.

4.) Derneryd, Anders G., "Analysis of the Microstrip Disk Element", IEEE Transactions on Antennas and Propagation, AP-27, No. 5, September, 1979.

5.) Howell, J.Q., "Microstrip Antennas", IEEE Transactions on Antennas and Propagation, AP-23, January, 1975.

6.) Carver, K.R., and Mink, James W., "Microstrip Antenna Technology", IEEE Transactions on Antennas and Propagation, AP-29, No. 1, January, 1981.

7.) Derneryd, Anders G., and Lind, Anders G., "Extended Analysis of Rectangular Microstrip Resonator Antennas", IEEE Transactions on Antennas and Propagation, AP-27, No. 6, November, 1979.

8.) James, J.R., 'Microstrip Antenna Theory and Design', Peter Pergrinus Ltd., London, 1981.